International Journal of Herbal Medicine
Available online at www.florajournal.com

E-ISSN: 2321-2187
P-ISSN: 2394-0514
www.florajournal.com
IJHM 2021; 9(5): 25-32
Received: 13-07-2021
Accepted: 15-08-2021

Ika Rahayu
(1) Biochemistry Department, Faculty of Medicine and Health Sciences, Universitas Kristen Krida Wacana (UKRIDA), Indonesia
(2) Research Center for Jamu and Herbal Medicine, Universitas Kristen Krida Wacana (UKRIDA), Indonesia

Kris Herawan Timotius
(1) Biochemistry Department, Faculty of Medicine and Health Sciences, Universitas Kristen Krida Wacana (UKRIDA)
(2) Research Center for Jamu and Herbal Medicine, Universitas Kristen Krida Wacana (UKRIDA), Indonesia

Corresponding Author:
Ika Rahayu
(1) Biochemistry Department, Faculty of Medicine and Health Sciences, Universitas Kristen Krida Wacana (UKRIDA)
(2) Research Center for Jamu and Herbal Medicine, Universitas Kristen Krida Wacana (UKRIDA), Indonesia

Antimutagenic and antiviral activity of hydroethanolic extract from *Moringa oleifera* L. leaves: *In vitro* and *in silico* studies

Ika Rahayu and Kris Herawan Timotius

Abstract
Moringa oleifera (MO) leaves have biological activities that are beneficial for improving health. *In vitro* studies show that its bioactive compounds prevent the development of some degenerative diseases. This study aimed to determine the bioactive compounds in hydroethanolic extracts of MO leave powder to measure its antioxidative and antimutagenic activity and to evaluate its ability to inhibit the SARS-CoV-2 main protease (Mpro) as a therapeutic target by in silico study. Liquid chromatography-mass spectrometry (LC-MS) was used to detect the bioactive compounds in hydroethanolic extract of MO leave powder. 2,2-Diphenyl-1-picrylhydrazyl (DPPH) was used to measure the antioxidant activity. The antimutagenic activity was measured by using the free radical treated plasmid pBR322. Molecular docking was used to determine the interaction of the bioactive compounds and the Mpro of SARS-CoV-2. Total phenolic and flavonoids compounds of MO leave powder hydroethanolic extract are 50.02±0.14 mg GAE/g and 445.07 ± 4.09 mg QE/g, respectively. The main bioactive compounds in the hydroethanolic extract are Guanine and Luteolin-7-O-glucoside. The antioxidant activity of hydroethanolic extract of leave powder is IC50 118.9 ± 0.2 µg/mL, which is stronger than the standard BHT IC50 11.60 ± 0.30 µg/mL. The MO hydroethanolic extract also has the ability to protect DNA damage. *In silico* studies show strong energy bonds of Mpro molecules with Guanine and Luteolin-7-O-glucoside, and the binding energy values are -6.2 and -8.4 kcal/mol, respectively. The hydroethanolic extract of MO leaf powder contains Guanine and Luteolin-7-O-glucoside. It has excellent antioxidant activity, and the ability to maintain DNA integrity or antimutagenic properties. As bioactive compounds, Guanine and Luteolin-7-O-glucoside, have the ability to attach Mpro of SARS-CoV-2. *In silico* study indicates that hydroethanolic extract of MO leave powder can act as a medicinal ingredient that has anti SARS-CoV-2 properties.

Keywords: auto dock, COVID-19; SARS-CoV-2, flavonoids, DNA-damage, Moringa

Introduction
Moringa oleifera (MO) is a nutrient-rich plant that can prevent nutritional deficiencies [1]. MO is rich in bioactive compounds that have antioxidant activity [2]. All parts of MO have biological activities that are beneficial for promoting health. The benefits include antidiabetic [3], antiallergic [4], hepatoprotective [5], anti-inflammatory and antiapoptotic activities [6]. *In vivo* study shows that MO bioactive compounds can improve testicular toxicity, injury, sperm count, abnormalities, and oxidative stress [7]. Free radicals and reactive oxygen species (ROS) are some sources of cellular and tissue pathogenesis. These can lead to the development of several diseases, such as diabetes, cancer, inflammation, atherosclerosis and cardiovascular disease. Free radical reactions that occur in the human body can cause damage and death [8]. Free radicals cause DNA damage or mutations. This damage involves the initiation phase of the carcinogenesis causing the cellular repair process to be incomplete [9, 10]. The accumulation of DNA damage is part of the ageing and degenerative diseases, such as diabetes [40]. During the current COVID-19 pandemic, many traditional medicines are used as alternative and complementary medicine to prevent and to treat COVID-19. Some of them have anti-inflammatory potentials, such as curcumin, 1.8 cineole and some other essential oils [12, 14]. Since MO has many health benefits, an *in silico* study can be conducted to explore the ability of its active compounds to interact with the main protease SARS-CoV-2 (Mpro). Accordingly, this research aimed to identify the bioactive compounds in hydroethanolic extract with liquid chromatography-mass spectrometry LC-MS to determine its antioxidant activity and ability to protect DNA from damage. Finally, we conducted an *in silico* study to determine the possible interaction between the bioactive compounds and the main protease SARS-CoV-2 (Mpro).

Materials and Methods

Sample preparation

Moringa oleifera leaf powder was obtained from CV. Kebonqta Mubarak, Jakarta. A total of 10g of MO was macerated using 300 mL of 80% ethanol. The result was filtered and then evaporated using an evaporator (Heidolph, Germany).

Total phenolic content

The total phenolic content of the extract was determined using Folin-Ciocalteau's reagent with Gallic acid as standard. A total of 0.5 mL of the sample was added to 2.5 mL of Folin-Ciocalteu's 10% reagent. After 10 minutes, 2.5 mL of 75 g/L Na_2CO_3 was added to the mixture. The reaction mixture was incubated for two hours at room temperature. Then, the absorbance of the reaction mixture was measured at 765 nm, and compared with a blank solution containing only solvent (500 µL). The total phenolic content was calculated as Gallic acid equivalent (GAE) from the calibration curve obtained from a standard solution of Gallic acid expressed GAE/g dry mass [15].

Total flavonoid content

Total dissolved flavonoid content was determined by the aluminum chloride colorimetric method. Quercetin was used to create the calibration curve. Fifty milligrams of Quercetin were dissolved in 95% ethanol and then diluted to make a standard curve. The diluted standard solution (0.5 mL) was mixed separately with 1.5 mL of 95% ethanol, 0.1 mL of 10% aluminum chloride, 0.1 mL of 1M sodium acetate and 2.8 mL of distilled water. After incubation at room temperature for 30 min, the absorbance of the reaction mixture was measured at 415 nm with a Biochrom Libra S22 spectrophotometer (UK). The number of samples was replaced with the same amount of distilled water in the blank [16].

Phytochemical analysis using Liquid Chromatography-Mass Spectrometry

LC-MS analysis was performed using Waters LCMS/MS-QTQF. The mode of operation uses Tof MSE, which was equipped with an ESI (Electrospray Ionization) source with positive and negative ion modes. The column used was column C18. The mobile phase used 0.1% formic acid in acetonitrile and 0.1% formic acid in distilled water (flow rate 0.6 mL/min). Ultrasonic for 30 minutes was done to homogenize 0.5 grams of sample and 10 mL of methanol, then filtered using a 0.22 m GHP/PTFE membrane filter. Finally, 10 µL filtrate was injected into the injection port. The screening process of the active substances was done using UNIFI software which has a mass spectrum library of natural active substances. The compound mass spectrum in the sample was then matched with the mass spectrum in the library. Active substances were identified if they met the following conditions: Mass error of analyte reading 5 ppm error, Isotope match MZ RMS 6, analyte intensity 300, there is one fraction with brake value < 4 in the Fragment elucidation system.

Antioxidant activity test with DPPH radical scavenging

A total of 500 µL extract at different concentrations was reacted with 1.500 µL DPPH 150 mM in absolute methanol. Incubation was done at room temperature in the dark for 30 minutes. The absorbance was measured at a wavelength of 517 nm using a spectrophotometer (Biochrome Libra S22). The radical quenching ability of DPPH was calculated using the following formula, where H and Ho were the optical densities of the solvent with and without the sample [17].

DNA protection activity test

DNA resistance to free radicals was measured using plasmids. The conversion of the supercoiled form of plasmid DNA into an open linear form was further used as an index of DNA damage. The following is the reaction mixture (15 µL); 5 µL of saline phosphate buffer (PBS, 10 mM, pH 7.4), 1 µL of plasmid DNA (0.5 g), 5µL of the sample, 2 µL of 1 mM $FeSO_4$, and 2 µL of 1 mM H_2O_2 and incubated at 37 °C for 30 min. The stop reaction, 2 µL of loading buffer (10 mM Tris-HCl pH 7.6, 60 mM EDTA 0.1% bromophenol blue, 0.1% xylene cyanol FF, 50% glycerol) was added after incubation. The reaction mixture was electrophoresed on a 0.85% agarose gel containing 0.5 µL of red gel [18].

In-Silico study of the active compound of MO leaves hydroethanolic extract with COVID-19 main protease.

The Main protease of SARS-CoV-2 virus (Mpro), a non-structural protein, was the target of the active compound in the MO hydroethanolic extract. Discovery Studio v21.1 and Pyrx 0.8 were used for all docking experiments. We used the Protein Data Bank to get the Mpro (Corona virus main protease in complex with an inhibitor N3, ID 6lu7).All bioactive compounds structures (ligands) was acquired from PubChem. Discovery Studio v21.1 was utilized to make the protein preparation: deleting waters and removing the N3 ligand. Ligands were modified into the most stable structure energetically using energy minimization. The ligand and protein molecules were converted to a readable file format (pdbqt) using Pyrx 0.8.

The docking was targeted to the active site of Mpro. The X, Y and Z values of the active site position were identified by Discovery studio. It was applied to create grid boxes in the docking process with Pyrx. The final visualization of the anchored structure was done by Discovery Studio Visualizer v21.1.

Data Analysis

Linear regression was used to analyze the antioxidant activity. Data was presented in Mean ± standard deviation (SD). Azzure software was used to analyze the antimutagenic activity.

Results and Discussion

The yield of the hydroethanolic extract of the MO leave measured as (w/w). LC-MS analysis of MO hydroethanolic extract detected one peak in positive ESI with a retention time of 0.38, and one peak in negative ESI with a retention time of 9.47 minutes (Figure 1, Table 1). Then for each fragmented peak, a positive ESI produced a fragmentation spectrum with a mass candidate (m/z) 107. At a negative ESI a fragmentation with a mass candidate (m/z) 447. Figure 1 and Table 2 show all of the compounds tentatively identified in the MO hydroethanolic extract in the positive and negative ionization modes. Detected Luteolin-7-O-glucoside, also known as 7-O-Glucoluteolin or Cinnacoside, is a class of flavonoid O-glycoside organic compounds. Luteolin-7-O-glucoside has strong antioxidant activity and anti-inflammatory activities [19], which protects against DNA damage [20]. Luteolin-7-O-glucoside can neutralize ROS-induced membrane damage and significantly improve the blood glucose profile, HbA1c, insulin and HOMA IR levels [21]. Luteolin-7-O glucoside is a promising antiviral candidates

[22, 24]. Guanine is a compound that resulted from the hydrolysis of Deoxynucleoside, a precursor to purine degradation. Guanine also produces Allantoin, Allantoin acid and CO2 [25]. Allantoin functions to protect plants from damage due to oxidative stress caused by ROS [26]. Allantoin able to protect the skin from irritation, to heal wounds, and to grow new tissue in damaged skin [27].

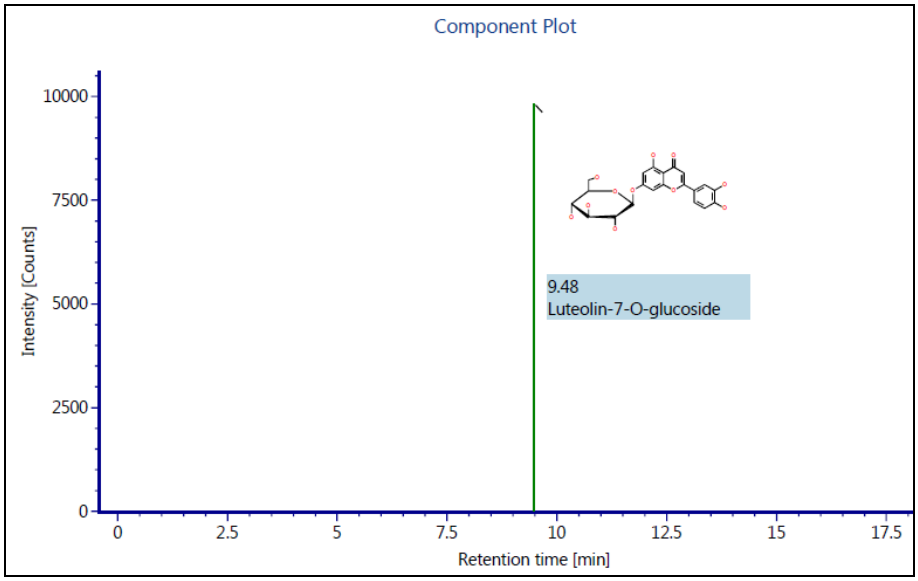

(a)

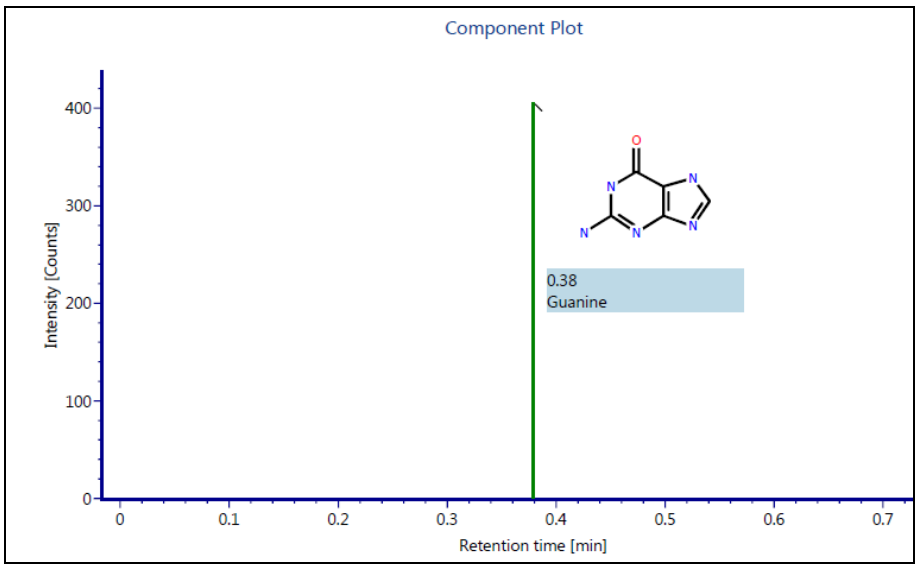

(b)

Fig 1: Bioactive compound Negative ESI (a) and Positive ESI (b)

Table 1: The bioactive compound of LCMS analysis

Compound	ESI Mode	RT	MZ	Response	Molecular Formula
Luteolin-7-O-glucoside	-	9.47	284 447	7528	$C_{21}H_{20}O_{11}$
Guanine	+	0.38	107 138 432	368	$C_5H_5N_5O$

The total phenolic and flavonoid content of the MO hydroethanolic extract are lower and higher, respectively, compared with the ethanol extract (Table 2) [28]. Analysis of the total flavonoid content showed that both extracts had high levels of flavonoids (Table 3). The relative percentage of flavonoids in MO hydroethanolic extract is high, as much as 89%.

Table 2: Total phenolic and flavonoid content.

Hydroethanolic extract	Concentration	Literature
Total phenolic content	50.02±0.14 mg GAE/g	This study
Total flavonoid content	44.51 ± 0.41 mg QE/g	This study
Ethanolic Extract		
Total phenolic content	63.16 mg GAE/g	[28]
Total flavonoid conten	10.477 mg QE/g	[28]

MO hydroethanolic extract can reduce free radicals, even ten times weaker than BHT. The IC50 of MO hydroethanolic extract and BHT were actually µg/mL and 11.60 ± 0.30 µg/mL, respectively. This result is in accordance with the opinion of Siddhuraju and Becker in 2003 and Nobose *et al*.in 2018 [29, 30].Their variation in antioxidants content depends on the kind of extraction solvent, maturity of the leaves, and growth environment [31, 33]. Antioxidants play an important

role in DNA damage protection. DNA damage is a consequence of oxidative stress. DNA damage occurs due to a variety of lesions, from isolated basic lesions or single-strand breaks (SSBs) to complex lesions such as double-strand breaks (DSBs) and also other non-DSB lesions such as clustered DNA lesions produced by oxidative reactions (OCDL). Inefficient repair of damage can result in cell injury and cause carcinogenesis [34, 35]. MO hydroethanolic extract has the ability to protect DNA from damage due to oxidative stress. The OH free radical generated from the Fenton reaction was reacted with the pBR322 plasmid. The pBR322 normal conformation is a supercoil (SC) with high electrophoretic mobility. When DNA reacts with radicals, it will cause the breaking of the double bond, which results in an open-loop conformation (OC) with low electrophoretic mobility. The separation of these two conformations can be seen by gel electrophoresis [36]. The MO hydroethanolic extract showed its ability to protect DNA at a concentration 15.75 mg/mL. Its ability is increased at a concentration of 37.5; 75; and 150 mg/mL. The OC conformation decreased by 75.31% at a concentration of 18.75mg/mL and 86.12% at concentration of 150 mg/mL (Table 3, Figure 2). The protective activity is strong because it restores the conformational condition, almost like the untreated plasmid.

Table 3: Antimutagenic analysis

Code	Treatment	OC (%)	Linear (%)	SC (%)
A	Plasmid +H_2O_2+Fe_2SO_4	95,22	4,7	0
B	0,58 mg/mL MO + Plasmid +H_2O_2+Fe_2SO_4	95,19	2,98	1,83
C	1,17 mg/mL MO + Plasmid + H_2O_2+Fe_2SO_4	85,63	7,81	6,55
D	2,34 mg/mL MO + Plasmid + H_2O_2+Fe_2SO_4	68,54	21,25	10,21
E	4,68 mg/mL MO + Plasmid + H_2O_2+Fe_2SO_4	40,85	44,25	14,89
F	9,37 mg/mL MO + Plasmid + H_2O_2+Fe_2SO_4	30,87	49,87	19,25
G	18,75 mg/mL MO + Plasmid + H_2O_2+Fe_2SO_4	19,91	57,27	22,82
H	37,5 mg/mL MO + Plasmid + H_2O_2+Fe_2SO_4	17,14	61,35	21,51
I	75 mg/mL MO + Plasmid + H_2O_2+Fe_2SO_4	13,86	65,92	21,21
J	150 mg/mL MO + Plasmid + H_2O_2+Fe_2SO_4	9,1	72,9	17,98
K	Non treatment Plasmid	3,1	70,78	26,07

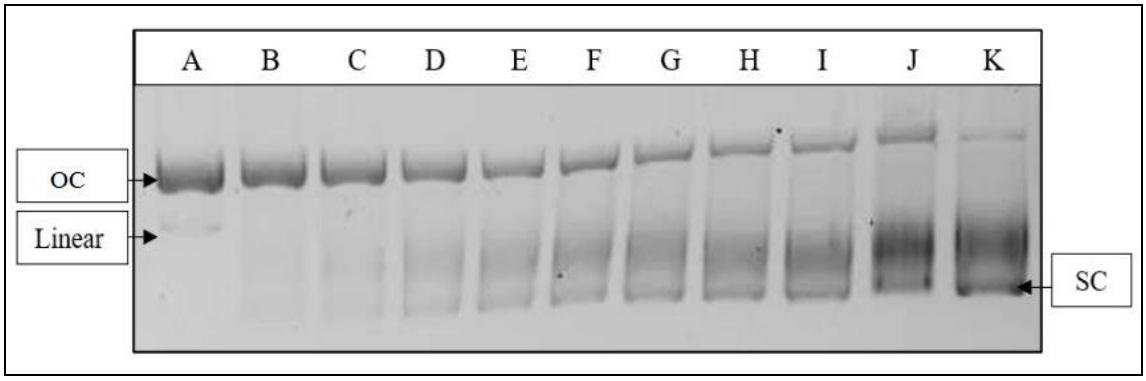

(a)

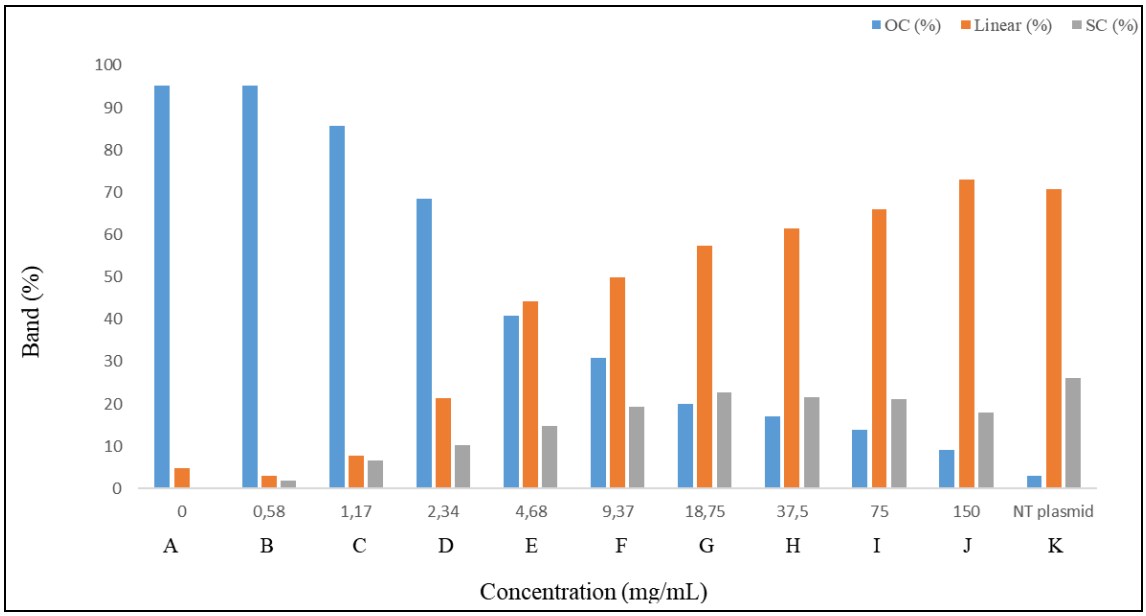

(b)

Fig 2: DNA protective effect of MO hydroethanolic extract.

Molecular docking was performed using a grid-based technique from Auto Dock Vina. Two ligands were attached to MPro SARS-CoV-2. The table shows the binding affinity of the ligand Guanine and Luteolin 7-O-glucoside with Mpro SARS-CoV-2 is -6.2 and -8.4 kcal/mol, respectively. Luteolin 7-O-glucoside showed the highest binding affinity to Mpro (Figure 3). These results are similar to the analysis of Khaerunisa *et al.*, 2020 [37]. Luteolin 7-O-glucoside has a higher affinity than Remdesivir and Guanine. Remdesivir was chosen as a comparison because it has shown the ability to shorten recovery time and reduce the incidence of respiratory tract infections in adults with COVID-19 [38].

Table 4: The best scores of the binding energy of the active compounds and the target proteins of Mpro

No	Active compound	Mpro (6lu7) (kcal/mol)	rmsd/ub	rmsd/lb
1	Luteolin-7-O-glucoside	-8.4	0.00	0.00
2	Guanine	-6.2	0.00	0.00
3	Remdesivir	-7.3	0.00	0.00

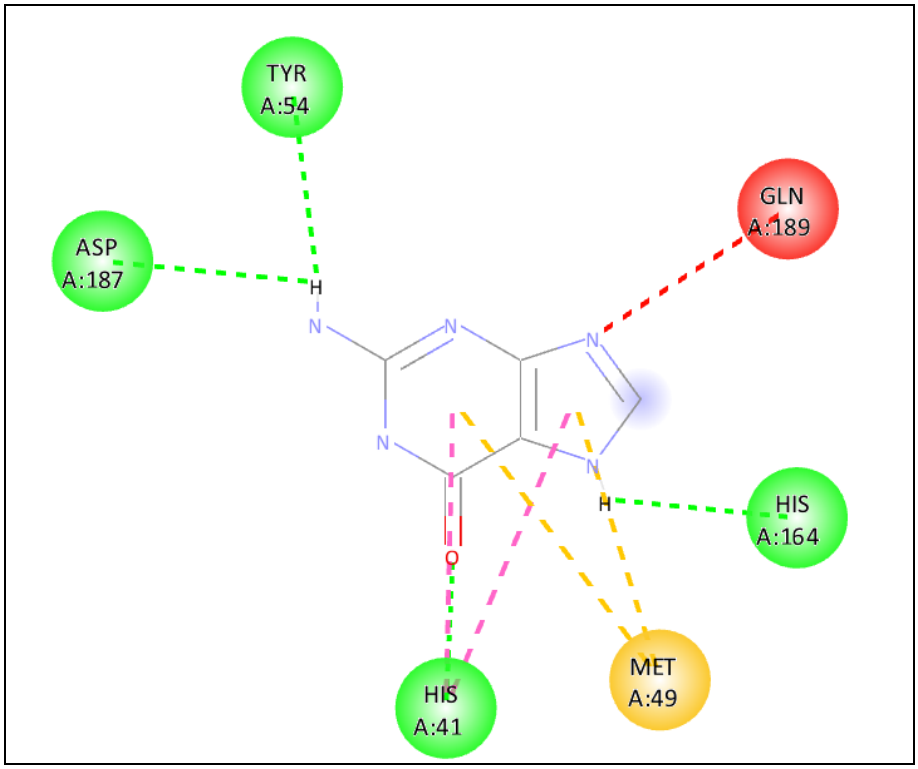

(a)

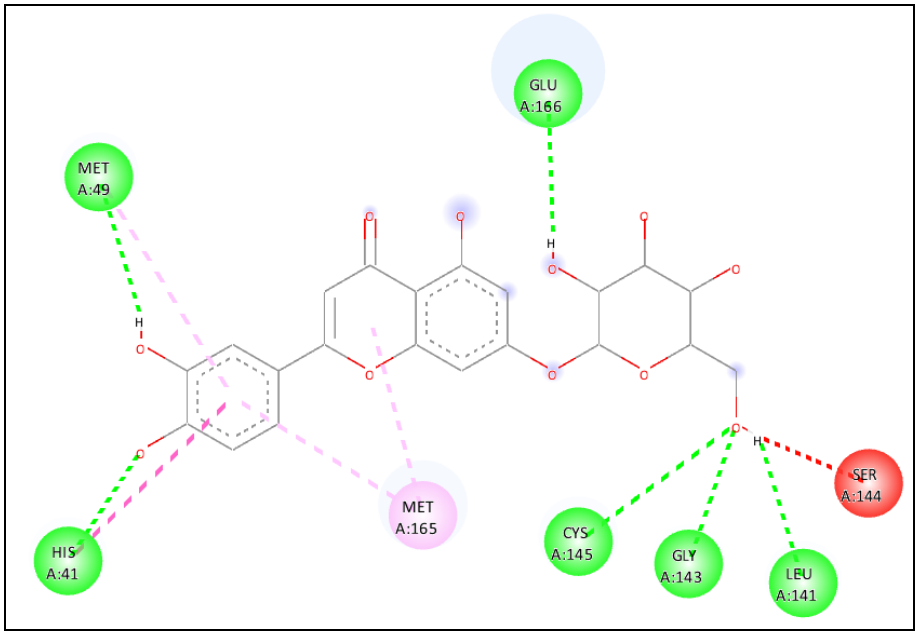

(b)

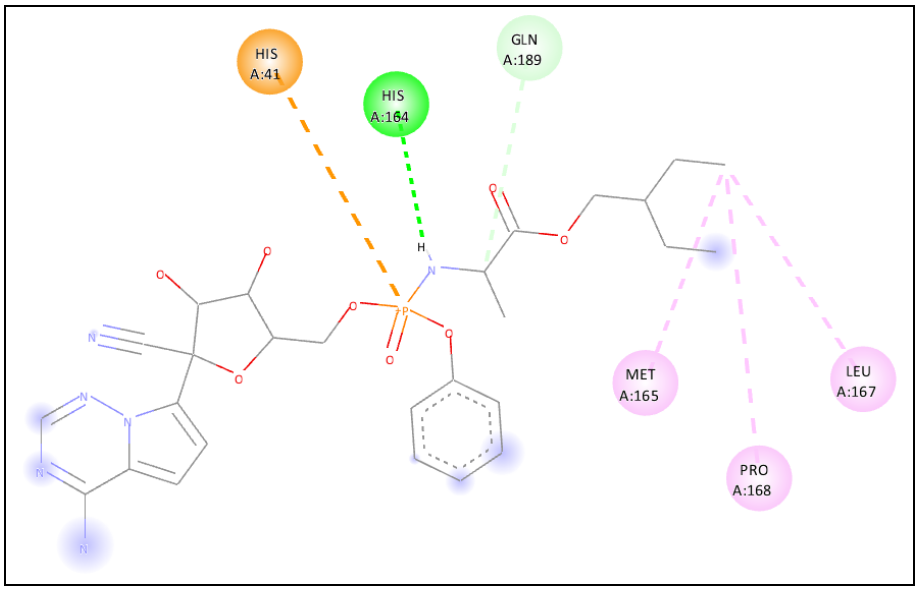

(c)

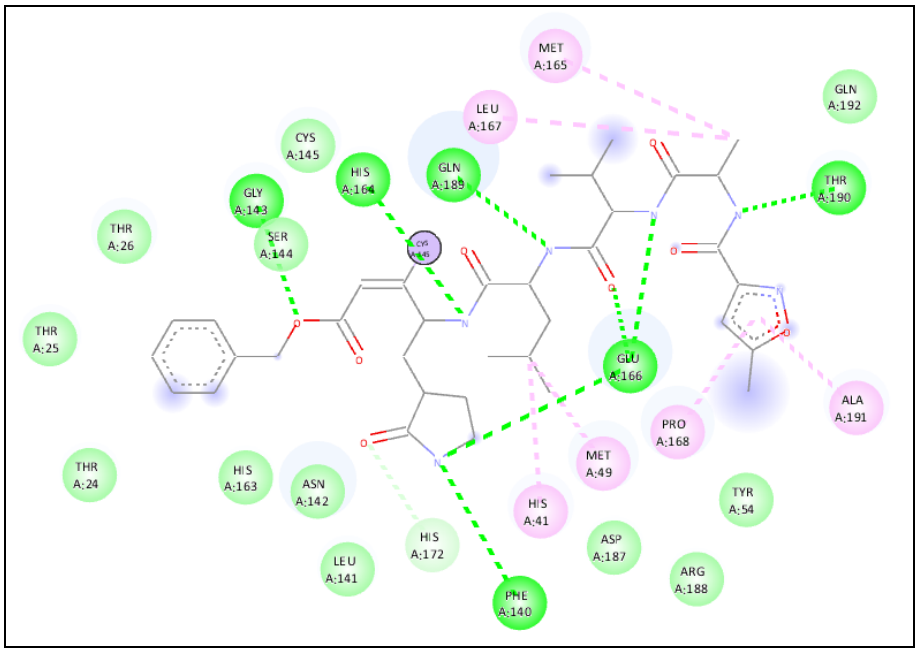

(d)

Fig 3: Results of Mpro docking with several active compounds in MO leaf hydroethanolic extract. (a). Mpro-guanine; (b). Mpro-luteolin-7-O-glucoside; (c). Mpro-remdesivir; (d). Mpro-N3 inhibitor

Detailed analysis of the best conformation was done using the free version of Biova Discovery Studio Visualizer. The interaction of Mpro with guanine has a bond free energy of -6.3 kcal/mol and an RMSD value of 0.000. Guanine binds to 6 residues, namely Gln189, His164, Met49, His41, Tyr54, Asp 187. Guanine interacts with the main protease with conventional hydrogen bonds at the residues Tyr54, Asp187, His41, His164, in addition to the stacked pi-pi bonds when interacting with His41. The pi-sulfur bond occurs at the Met49 residue with Guanine. Unfavorable acceptors occur in interactions with Gln189 residues.

The interaction of Mpro with Luteolin 7-O-glucoside has bond-free energy of -8.4 kcal/mol and RMSD of 0.000. Luteolin 7-O-glucoside binds to 8 amino acid residues, namely Glu166, Met49, His41, Met165, Cys145, Gly143, Leu141, Ser 144. Interaction between Luteolin 7-O-glucoside and Met165 with Pi-alkyl bonds. Unfavorable donor-donor interactions occur with the Ser144 residue. The p-alkyl bond occurs in the interaction of Luteolin 7-O-glucoside with Met165. Other residues interact with conventional hydrogen bonds.

The interaction between Mpro and Remdesivir has a bond free energy of -7.3 kcal/mol and RMSD of 0.000. Remdesivir binds to 6 amino acid residues, namely Gln189, His164, His41, Met165, Pro168 and Leu167. The interaction between Remdesivir and residues of Met165, Pro168 and Leu167 is through the Pi-alkyl bond. The pi-cation binding occurs on the interaction of Remdesivir with the His41 residue. Remdesivir is bound to the Gln189 residue by a carbon-hydrogen bond, and to His164 by a conventional hydrogen bond.

These three compounds bind stably to the target protein (Mpro) and appear to have a mechanism that comparable to N3 inhibitors [39]. This can be indicated by the binding of several residues such as Met165, Leu167, Pro168, Gln189, Tyr54, Asp187, Met49, His41, and His164 to each compound. Accordingly, it can be concluded that Guanine and Luteolin

7-O-glucoside may be used as SARS-CoV-2 antiviral candidates [37].

Conclusion

The bioactive compounds of the MO hydroethanolic extract are Luteolin-7-O glucoside and Guanine. MO Hydroethanol extract has antioxidative activity even weaker than BHT. However, MO hydroethanol extract has good potential applications in DNA protection activity. The bioactive compounds, Luteolin-7-O glucoside and Guanine are potential candidates as antiviral agents.

Recommendations

Further studies on MO leave extracts are necessary to confirm their efficacy, particularly in the protective activity against DNA damage, as an anticancer and antiviral agent.

Acknowledgements

This work was supported by the Research and Community Institute of Universitas Kristen Krida Wacana (LPPM-UKRIDA).

References

1. Mbikay M. Therapeutic Potential of *Moringa oleifera* Leaves in Chronic Hyperglycemia and Dyslipidemia: A Review. Frontier in Pharmacology 2012;3:1-12.
2. Airouyuwa JO, Kaewmanee T. Microencapsulation of *Moringa oleifera* leaf extracts with vegetable protein as wall materials. Food Science and Technology International 2019;25(6):533-534.
3. Aa AB, Om J, Ts E, Ga A. Preliminary phytochemical screening, antioxidant and antihyperglycaemic activity of *Moringa oleifera* leaf extracts. Pakistan Journal of Pharmaceutical Sciences 2017;30(6):2217-2222.
4. Abd Rani NZ, Kumolosasi E, Jasamai M, Jamal JA, Lam KW, Husain K. *In vitro* antiallergic activity of *Moringa oleifera* Lam. extracts and their isolated compounds. BMC Complementary Medicine and Therapies 2019;19(361):1-16.
5. Abdel Fattah ME, Sobhy HM, Reda A, Abdelrazek HMA. Hepatoprotective effect of Moringa oleifera leaves aquatic extract against lead acetate-induced liver injury in male Wistar rats. Environmental Science and Pollution Research 2020;27(34):43028-43043.
6. Abdel-Daim MM, Khalil SR, Awad A, Abu Zeid EH, El-Aziz RA, El-Serehy HA. Ethanolic Extract of Moringa oleifera Leaves Influences NF-κB Signaling Pathway to Restore Kidney Tissue from Cobalt-Mediated Oxidative Injury and Inflammation in Rats. Nutrients 2020;12(4):2-20.
7. Abdou KH, Moselhy WA, Mohamed HM, El-Nahass ES, Khalifa AG. *Moringa oleifera* Leaves Extract Protects Titanium Dioxide Nanoparticles-Induced Nephrotoxicity via Nrf2/HO-1 Signaling and Amelioration of Oxidative Stress. Biological trace element research 2019;187(1):181-191.
8. Halliwell B. Are polyphenols antioxidants or pro-oxidants? What do we learn from cell culture and *in vivo* studies?. Archives of Biochemistry and Biophysics 2008;476(2):107-112.
9. Johnson IT. Phytochemicals and cancer. Proceedings of the Nutrition Society 2007;66(2):207-215.
10. Basu AK. DNA Damage, Mutagenesis and Cancer. International journal of molecular sciences 2018;19(4):1-13.
11. Sruthi N, Nithyasree R, Sathya A. Drug reposition of Amoxycillin by molecular docking. Int. J Adv. Chem. Res. 2020;2(2):01-11. DOI: 10.33545/26646781.2020.v2.i2a.21
12. Ryu Y, Jeong H, Kim J, Kim YM, Park JY, *et al*. Biflavonoids from *Torreya nucifera* displaying SARS-CoV 3CL(pro) inhibition. Bioorganic and Medicinal Chemistry 2010;18(22):7040-7047.
13. Asif M, Saleem M, Saadullah M, Yaseen HS, Al Zarzour R. COVID-19 and therapy with essential oils having antiviral, anti-infammatory, and immunomodulatory properties. Inflammopharmacology 2020;28(5):1153-1161.
14. Sharma AD, Kaur I. Eucalyptol. (1,8 cineole) from Eucalyptus Essential Oil a Potential Inhibitor of COVID 19 Corona Virus Infection by Molecular Docking Studies. Preprints 2020, 1-8.
15. Shukla S, Park J, Kim DH, Hong SY, Lee JS, Kim M. Total phenolic content, antioxidant, tyrosinase and α-glucosidase inhibitory activities of water soluble infusions of noble starter culture Doenjang, a Korean fermented soybean sauce variety. Food Control 2016;59:854-861.
16. Chia-Chi C, Ming Hua Y, Hwei-mei W, Jiing-Chuan C. Estimation of total flavonoid content in propolis by two complementary colorimetric methods. Journal of food and drug analysis 2002;10:178-182.
17. Singleton VL, Orthofer R, Lamuela-Raventós RM. Analysis of total phenols and other oxidation substrates and antioxidants by means of Folin-Ciocalteu reagent. Methods in Enzymology 1999;299:152-178.
18. Jeong JB, Park JH, Lee HK, Ju SY, Hong SC, Lee JR, *et al*. Protective effect of the extracts from *Conidium officinale* against oxidative damage induced by hydrogen peroxide via antioxidant effect. Food and Chemical Toxicology 2009;47(3):525-529.
19. Cui XX, Yang X, Wang HJ, Rong XY, Jing S, Xie YH, *et al*. Luteolin-7-O-Glucoside Present in Lettuce Extracts Inhibits Hepatitis B Surface Antigen Production and Viral Replication by Human Hepatoma Cells *in Vitro*. Frontiers in Microbiology 2017;8:1-12.
20. Boldbaatar D, El-Seedi HR, Findakly M, Jabri S, Javzan B, *et al*. Antigenotoxic and antioxidant effects of the Mongolian medicinal plant *Leptopyrum fumarioides* (L): An *in vitro* study. Journal of ethnopharmacology 2014;155(1):599-606.
21. Yanqing Z, Kiharu I, Yu L. Antidiabetic effects of luteolin and luteolin-7-O-glucoside on KK-Ay mice. Bioscience, Biotechnology and Biochemistry 2016;80(8):1580-1586.
22. Beladi I, Pusztai R, Mucsi I, Bakay M, Gabor M. Activity of some flavonoids against viruses. Annals of the New York Academy of Sciences 1977;284:58-364.
23. Xiao-Xian C, Xiao Y, Hui-jing W, Xing-Yu R, Sha J, You-Hua X. Luteolin-7-O-Glucoside Present in Lettuce Extracts Inhibits Hepatitis B Surface Antigen Production and Viral Replication by Human Hepatoma *Cells in Vitro*. Frontier Microbiology 2017;8:1-12.
24. Flores-Ocelotl MR, Rosas-Murrieta NH, Moreno DA, Vallejo-Ruiz V, Reyes-Leyva J, Domínguez F, *et al*. Taraxacum officinale and Urtica dioica extracts inhibit dengue virus serotype 2 replication *in vitro*. BMC Complementary and Alternative Medicine 2018;18(1):1-10.
25. Wei-Wei D, Katahirab R, Ashihara H. Short Term Effect

of Caffeine on Purine, Pyrimidine and Pyridine Metabolism in Rice (*Oryza sativa*) Seedlings. Natural product communications 2015;10(5):737-741.
26. Watanabe S, Kounosu Y, Shimada H, Sakamot A. Arabidopsis xanthine dehydrogenase mutants defective in purine degradation show a compromised protective response to drought and oxidative stress. Plant biotechnology journal 2014;31:1-6.
27. Elżbieta S. Allantoin – healing and anti-inflammatory properties. Pediatria i Medycyna Rodzinna 2012;8(1):73-77.
28. Fachriyah E, Kusrinia D, Haryanto IB, Wulandari SMB, Lestari WI, Sumariyah. Phytochemical Test, Determination of Total Phenol, Total Flavonoids and Antioxidant Activity of Ethanol Extract of *Moringa* Leaves (*Moringa oleifera* Lam). Jurnal Kimia Sains dan Aplikasi 2020;23(8):290-294.
29. Siddhuraju P, Becker K. Antioxidant Properties of Various Solvent Extracts of Total Phenolic Constituents from Three Different Agroclimatic Origins of Drumstick Tree (*Moringa oleifera* Lam.) Leaves. Journal of Agricultural and Food Chemistry 2003;51(8):2144-2155.
30. Nobossé P, Fombang EN, Mbofung CMF. Effects of age and extraction solvent on phytochemical content and antioxidant activity of fresh *Moringa oleifera* L. leaves. Food Science and Nutrition 2018;6(8):2188-2198.
31. Ahmed E, Shaker OG, Yussif N, Ghalwash DM. Effect of Locally Delivered Melatonin as an Adjunct to Nonsurgical Therapy on GCF Antioxidant Capacity and MMP-9 in Stage II Periodontitis Patients: A Randomized Controlled Clinical Trial. International journal of dentistry 2021, 1-9.
32. Adebayo IA, Arsad H, Samian MR. Total Phenolics, Total Flavonoids, Antioxidant Capacities, and Volatile Compounds Gas Chromatography-Mass Spectrometry Profiling of *Moringa oleifera* Ripe Seed Polar Fractions. Pharmacognosy magazine 2018;14(54):191-194.
33. Fitria D, Scholz M, Swift GM. Impact of different shapes and types of mixers on sludge dewaterability. Environmental technology 2013;34(5-8):931-936.
34. Tiwari P, Mishra. Role of Flavonoids in DNA Damage and Carcinogenesis Prevention. Journal of carcinogenesis and mutagenesis research 2017;8(4):1-6.
35. Sabahi Z, Soltani F, Moein M. Insight into DNA protection ability of medicinal herbs and potential mechanisms in hydrogen peroxide damages model. Asian pacific journal of tropical biomedicine 2018;8(2):120-129.
36. Chatsumpun M, Chuanasa T, Sritularak B, Likhitwitayawuid K. Oxyresveratrol Protects Against DNA Damage Induced by Photosensitized Riboflavin. Natural product communications 2011;6(1):41-44.
37. Khaerunnisa S, Kurniawan H, Awaluddin R, Suhartati S, Soetjipto S. Potential Inhibitor of COVID-19 Main Protease (Mpro) From Several Medicinal Plant Compounds by Molecular Docking Study. Preprints 2020;1:1-9.
38. Beigel JH, Tomashek KM, Dodd LE, Mehta AK, Zingman BS, Kalil AC. Remdesivir for the Treatment of COVID-19 - Final Report. The New England Journal of Medicine 2020;383(19):1813-1826.
39. Zhenming J, Xiaoyu D, Yechun X, Yongqiang D, Eiqin L, Yao Z, *et al.* Structure of Mpro from SARS-CoV-2 and discovery of its inhibitors. Nature 2020;482:289-304.
40. Shimizu I, Yoshida Y, Suda M, Minamino T. DNA damage response and metabolic disease. Cell metabolism 2014;20:967-977.